ELECTROMECHANICAL PROPERTIES OF CARBON NANOTUBE BUCKYPAPERS

M D Rein[1,2], H Bar[1], O Breuer[1], R Yoseph[1] and H D Wagner[2]
[1]Rafael – Advanced Defense Systems Ltd, POB 2250, Haifa 31021
[2] Department of Materials and Interfaces, The Weizmann Institute of Science, Rehovot 76100, Israel
Michael.Rein@weizmann.ac.il

SUMMARY

The electrical resistance of single and multi-walled carbon nanotubes buckypaper films was studied as a function of mechanical strain. The buckypaper strain sensors were encapsulated in epoxy matrices and the effect of carbon nanotube type and degree of strain on their resistance change and sensitivity were studied.

Keywords: Buckypaper, sensor, electromechanical, high strain, nanotubes

INTRODUCTION

Mechanical and electrical properties of carbon nanotubes (CNTs) make them promising materials for development of novel smart composites. Both single-walled CNTs (SWCNTs) and multi-walled CNTs (MWCNTs) were found to exhibit a reversible relationship between their mechanical deformation and the electrical resistance [1-3] thus it is possible to imply that CNTs could be used as a precise strain or stress sensors. These exciting properties may lead to a new generation of materials for building enhanced strain sensors both at the micro and macro scales. Several studies [2,3] had shown that direct dispersion of CNTs in the composites' polymer allows using the material as strain sensors for structural health monitoring. Additional approach that was initially utilized by Dharap et. al. [1] is to use CNTs films as strain sensors if they are bonded to a surface of some structure. This study showed that there is a nearly linear relationship between the measured change in voltage and the strains in the films.

Investigation of the electromechanical properties of carbon nanotubes in the form of buckypaper has several advantages. First, it eliminates the problem of achieving homogeneous nanotube dispersion, which is a major problem with nanocomposite strain sensing materials. Second, buckypaper films form isotropic and dense packed array of nanotubes, which enables to achieve high sensitivity and isotropic behaviour of the strain sensor, in contrast to conventional strain gauges.

Although recent studies had shown that buckypaper (BP) films could be utilized as stress sensors, the electromechanical properties of these films are as yet not well understood. The purpose of the current research was to investigate the electrical and mechanical properties of films composed of SWCNTs and MWCNTs, the coupling between those properties, and to assess the possibility to use these materials as strain sensors.

EXPERIMENTAL

Buckypaper preparation procedure:

25 mg of pristine SWCNT (D1L110-P, supplied by Nano-Lab, USA) or pristine MWCNT (PD30L520, same supplier) were stirred in 100ml of Dimethylformamide (DMF) solvent (Sigma Aldrich, Germany) for 6 hours. The stirring was followed by ultrasonication in a bath sonicator (MRC DC-80H, 80W, Israel) for 3 hours and by an ultrasonic tip (Sonics, Vibra-Cell VCX130, USA) for 20 minutes. Right after the dispersion process was finished, the solution was poured onto a 0.45 μm pores diameter Nylon filtration membrane (Sigma – Aldrich, Germany), and filtrated by a vacuum filtration setup. The filtered nanotubes were washed with distilled water several times, dried in vacuum oven which was preheated to ~60^{o}C for 12hrs. The freestanding BP film was peeled off the membrane after the drying process was complete.
Scanning electron microscopy (SEM) images of the resulting SWCNT and MWCNT BP films are shown in Figures 1 and 2.

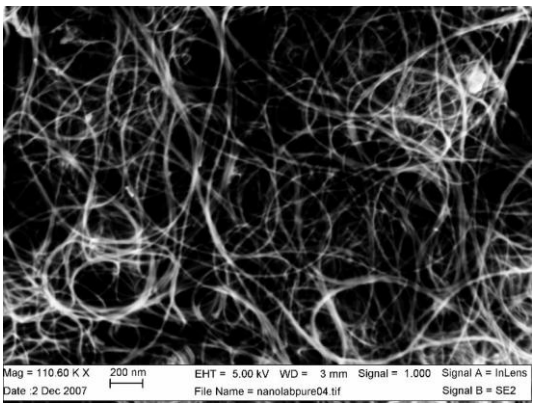

Figure 1 – SEM image of MWCNT BP

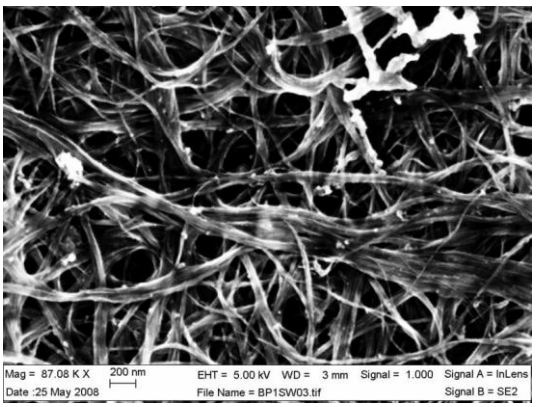

Figure 2 – SEM image of SWCNT BP

BP strain sensor preparation method:

Measurements of direct current (DC) surface resistance and electromechanical properties of all BPs were made by four point probe method. Small square pieces (length of ~10mm, width of ~4mm) of BP were cut (both from MWCNT and SWCNT) BPs. Copper wires with a diameter of 0.2mm were suspended on a specially designed holder, and adhered to the BP surface with a silver paint (High Purity Silver Paint, SPI supplies). Four wires were glued on the surface of the BP. All sensors were encapsulated into epoxy matrices. The purpose of the encapsulation was to achieve a homogeneous deformation of the BP sensor, by applying tensile stress/strain on the polymer material and to provide protection to the sensor and to the attached electrodes during mechanical deformation. The sensor was located in the middle of a tensile specimen, as described in Figure 3.

Three different epoxy polymers were used in order to prepare composite specimens. Polymer 1 - Epon 815C epoxy resin (Miller Stephenson Co., USA) based on n-butyl glycidyl ether bisphenol – A was mixed with Versamid 140 polyamide resin hardener (Miller Stephenson Co., USA) in a ratio of 70:30. This polymer exhibits relatively brittle behavior - high tensile modulus (2.2 GPa), strength of 38 MPa and a relatively low strain to failure (~1.5%).

Polymer 2 which was used - transparent rubberized epoxy resin ER2037 (Crosslink Technologies Inc., USA), based on n-butyl glycidyl ether bisphenol – A, with CT2037 hardener. Mixing ratio of 50:50 was used. This polymer exhibits very flexible behavior - low tensile modulus (16 MPa), low strength – 3 MPa but an extremely high strain to failure (~40%).

All polymer matrices were cured at room temperature for 48 hour, followed by a post curing heating process at 60^{o}C for additional 24hrs.

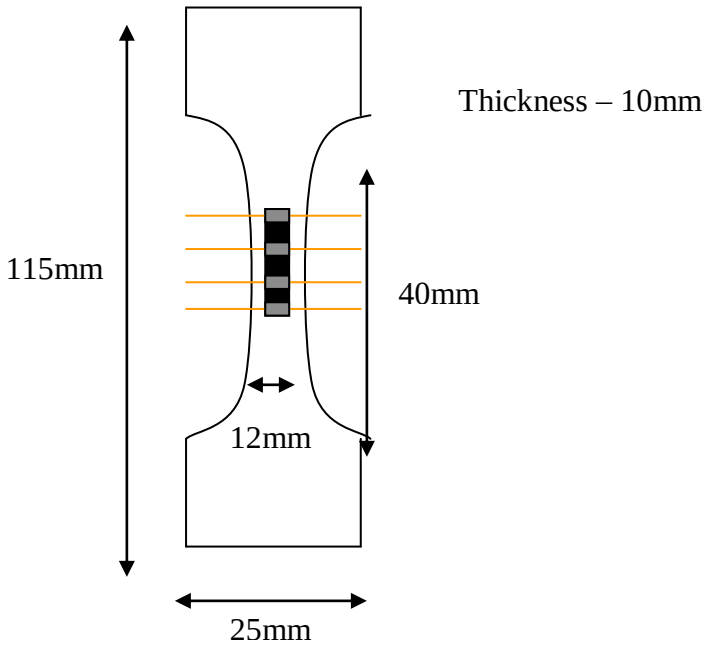

Figure 3 – Composite tensile specimen with incorporated BP sensor

Characterization methods

SEM images were taken by High Resolution Scanning Electron Microscopy (HRSEM) Zeiss Leo SUPRA 55VP, with an accelerating voltage of 5 KV and a working distance of 3-6 mm. DC resistance measurements of BPs were accomplished by 4 contact wire measurement method, in order to eliminate the effect of contact resistance. A current was applied on the two outer electrodes of the BP sensor by SourceMeter 2400 (Keithley, USA) and the resulting voltage was measured between the two inner electrodes by the same equipment. The resistance measurements were performed with varying mechanical deformations and currents. The specimen was mounted on a tensile test machine (Instron 5500R, UK), with load capacity up to 100KN. The extension of the specimen was measured by a non contacting video extensometer (Instron SVE, UK) between two dots which were administered on the specimen (with gauge length of 25mm). At least 4 specimens of each type were prepared and characterized.

RESULTS AND DISCUSSION

SWCNT and MWCNT BP characterization

MWCNT were homogenously dispersed in the film and no apparent rope formation was observed, as a continuous network of nanotubes was formed during the BP preparation sequence. Similar analysis was performed for SWCNT BPs which showed that SWCNTs were not fully dispersed, and formed bundled structures. This feature was not surprising, as many other works showed that this phenomenon is very common, especially among single-walled carbon nanotubes [4, 5]. The reason for these bundles formation is the presence of attractive van der Waals interactions which are highly favorable for SWCNTs. The mean diameter of MWCNT in MWCNT BP was 30±5nm and the thickness of the film was $72 \pm 4\mu m$. For SWCNT BP the mean bundle diameter was 68 ± 25 nm with the film thickness of $67 \pm 4\mu m$. Assuming the densities of MWCNTs to be ~2.25 gr/cm^3 and the density of SWCNTs ~1.3 gr/cm^3, the volume fractions of the nanotubes in the BPs were calculated. The resulting volume fraction of MWCNT in its BP film was 8.9% and the volume fraction of SWCNT in its BP film was 16.5%. Both MWCNT and SWCNT were highly porous, although the volume fraction of SWCNT was higher due to the low density of the SWCNTs.

The MWCNT and SWCNT BP differed not only in their volume fraction, but in their resistivity as well. The resistivity of MWCNT BP was found to be $(1.6\pm0.7)\cdot10^{-3}$ Ω·m and the resistivity of SWCNT BP was $(9.3\pm4)\cdot10^{-5}$ Ω·m. The resistivity was measured by a 4-wire technique, MWCNT BP resistivity was measured with a current of 1mA, and the resistivity values of SWCNT BP was measured with a current of 10mA.

The resistivity values of MWCNT and SWCNT BPs could be compared to values reported in other references. Resistivity of MWCNT was found to be in the range of 10^{-4}-10^{-3} Ω·m, [6,7] while the resistivity of SWCNT was found to be within the range of $1.8\cdot10^{-5}$- $6\cdot10^{-5}$ Ω·m. [8,9]

While both the resistivity values of MWCNT and SWCNT buckypapers fall in the range of the resistivity values seen in the literature discrepancies maybe explained by different production techniques which were used to prepare both the MWCNT and the SWCNT, different concentration of the nanotubes in the solvent, different nanotubes diameter and length, and/or different film morphology. Lyons et al. [8] had shown that those properties are crucial factors in determination of BPs' resistivities. SWCNT BP resistivity is ~16.7 times higher than the resistivity of MWCNT film. Two main factors control charge transport through BP films: the resistivity of the tubes themselves and the contact resistance between the nanotubes, where tunneling effects control the contact electrical behavior. The intrinsic resistivity might be affected by the conducting or semiconducting type of the nanotube, diameter distribution of the NTs, and structure defects [10]. The contact resistivity is affected by the morphology of the BP: the area of contact between nanotubes or nanotubes bundles, and the distance between adjacent contacts. Although the intrinsic resistivities depend on the NTs diameters and lengths, the highest resistivity values observed for metallic SWCNT was ~10^{-6} ohm·cm, and for MWCNT ~$4\cdot10^{-6}$ ohm·cm. [11,12] Thus the resistivity values of the BP films arising solely from intrinsic MWCNT or SWCNT resistivities are considerably lower than the resistivity of the BPs obtained in this research. Thus it is possible to rule out the contribution of the intrinsic resistivity of CNTs. The main factors which contribute to the resistivity of BP films are the contacts between nanotubes and nanotube bundles.

The differences in resistances could then arise from different contact area between the nanotubes (Contact area between MWCNT is bigger, as the diameter of the MWCNT is higher than the diameter of SWCNTs), the total number of contacts or the density of the contacts (SWCNT BP have higher number of contacts as the volume fraction of SWCNT in the BP is higher) and the number of contacts along the current pathway.

Electromechanical properties of MWCNT and SWCNT BPs

The electromechanical properties of MWCNT and SWCNT BP sensors were assessed by performing various tensile tests on the encapsulated specimens. The main variables which were changed between the experiments were: NT type (SWCNT or MWCNT); polymer matrix (Polymer 1 or 2); type of loading (cyclic or tension until failure); and the measuring current. The resistance change was defined by:

$$R_{change}(\%) = \frac{R - R_0}{R_0} \cdot 100 \quad (1)$$

where R is the resistance measured at a particular moment, R_0 is the initial resistance of the sensor. The results are presented in the figures of Table 1. The electrical resistance of the sensors closely follows the strain data collected by the video extensometer, thus experimentally confirming that both MWCNT and SWCNT BP sensors are sensitive to strain and possess sensing features. The BP sensors are able to measure strains of materials with different mechanical properties (stiffness, modulus of elasticity).

It is possible to notice that the resistance change as a function of strain of SWCNT BP sensors are very similar to MWCNT BP sensors, and this property will be assessed quantitatively later on. When comparing the results obtained for the different polymer matrices, we could see that resistance change occurs in the same manner and degree for polymer 1 and 2, regardless to the stress applied on the material. Assuming that the MWCNT or SWCNT BP sensor is tightly adhered to the polymer matrix (as shown in Figure 4), the resistance change occurs even when extremely low stress is applied on the sensor. SEM analysis of the BP-polymer matrix interface was performed in order to assess the interaction between the polymer matrices and the BP sensor. **Figure** clearly shows that the interface between the polymer matrix and the BP sensor shows no existence of defects or delaminating, which could affect the stress transfer from the polymer to the BP sensor.

Furthermore, it is possible to recognize that the polymer matrix fully penetrated into the pores which are present in the BP sensor. Thus we can assume that the stress and strain are fully transferred from the matrix to the BP sensor. Taking these facts into account we may suggest that the electromechanical behavior of the sensors are most probably governed by the morphological and geometrical properties of the sensors, and it is most likely that the intrinsic piezoresistive properties of the nanotubes play a minor role in the piezoresistive properties of both SWCNT and MWCNT sensors. It is possible to notice that the resistance change doesn't fully follow a linear dependency, although linear approximation between the resistance change and strain is possible and yields good results. Non linearity is apparent even for the most elastic matrix – polymer 1, which suggests that the resistance change of the sensor is intrinsically non linear, and not induced solely by the inelastic polymer behavior.

Table 1 - Stress and Resistance change as a function of strain for different BP types and polymer matrices, low strain loading (cyclic)

	MWCNT BP sensor	**SWCNT BP sensor**
Polymer 1	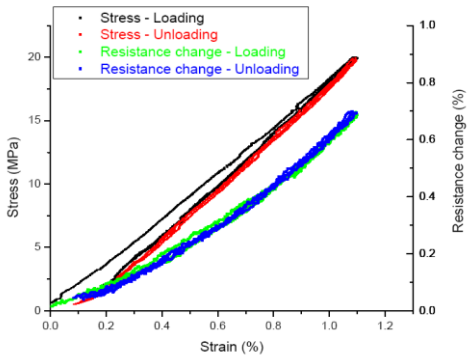	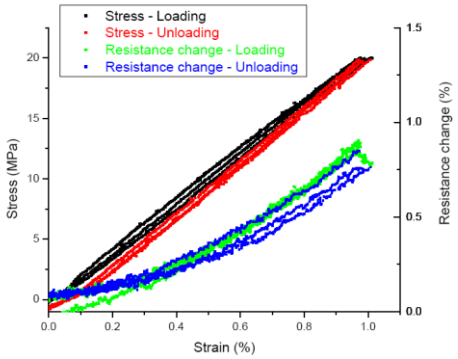
Polymer 2	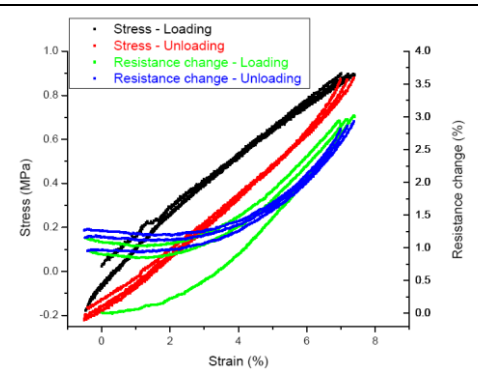	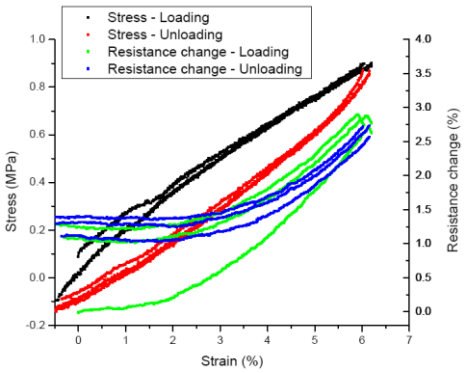

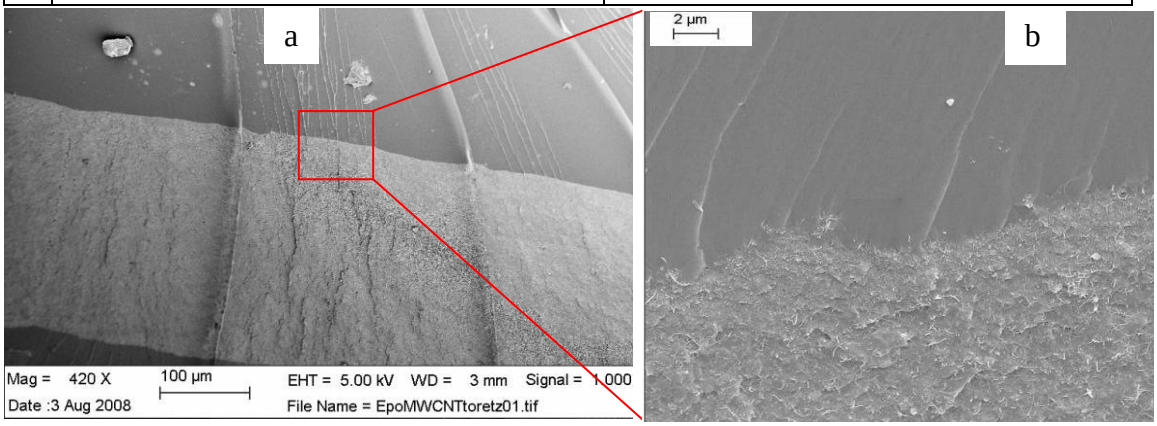

Figure 4 - SEM micrographs of MWCNT BP sensor - polymer 1 interface. a) Small magnification of the interface area. The polymer is on the top of the figure; b) Large magnification of the area indicated by the red square.

Non linear behavior was discovered for composite materials with SWCNTs and MWCNTs dispersed in polymer matrix [13, 14]. In this case the behavior can be approximated to an exponential dependency and it was attributed to the tunneling resistance between the conductive particles, which is known to depend exponentially on the inter-particle distance [14]. The latter explanation to the non linear

electromechanical behavior seems to be more precise, and an exponential fit between the resistance change as a function of strain gives better results compared to a linear fit. Nevertheless, exponential fit doesn't allow performing an effective comparison between the electromechanical measurements made in this study, thus linear approximation was held.
Furthermore, resistance values which could be relatively easily measured, doesn't represent direct physical properties of the BP sensors due to the effect of geometrical change of the sensor during loading. Thus the resistivity should be calculated for all specimens in order to receive physical understanding of the processes which occur during straining of the BP sensors.

In order to compare between the tests made herein - the sensitivity (S) of the sensors were calculated by the linear approximation made for the resistance change with strain upon loading and unloading.

$$(2) \quad S = \frac{\Delta R_{change}}{\Delta \varepsilon}$$

The calculated sensitivities upon loading and unloading are listed in **Table** :

Table 2 – Sensitivity of the BP sensors

	MWCNT BP sensor		**SWCNT BP sensor**	
	Loading	**Unloading**	**Loading**	**Unloading**
Polymer 1	0.86 ± 0.1	0.79 ± 0.14	2.2 ± 0.4	2.1 ± 0.4
Polymer 2	0.69 ± 0.1	0.6 ± 0.07	0.6 ± 0.1	0.59 ± 0.1

As could be seen from Table , the type of CNT and the type of the polymer matrix affect the resulting sensitivity of the electric resistance to strain. The sensitivity of SWCNT sensors is different from the sensitivity of MWCNT sensors incorporated into polymer 1, although the difference is less prominent for polymer 2. We suggest that the difference in the sensitivity of the BPs in polymer 1 is influenced by the interaction between the polymer and the sensor. Factors such as stress transfer between the polymer and the sensor, or the stress which is required in order to introduce a change into the BP mesh, could affect the electromechanical properties of the sensors. Although no unambiguous explanation could be provided based on these results, it is important to notice that the type of BP sensor (MWCNT and SWCNT) could not solely describe its electromechanical behavior and the interaction between the polymer matrices with BP sensors plays an important role when utilizing BP films as strain sensors.
Comparison of the absolute sensitivity values of the sensors to values obtained for metallic strain gauges, other SWCNT BP films and composite materials containing CNT as reinforcements shows that the sensitivities of both SWCNT and MWCNT BP strain sensors are in the same order of magnitude as the sensitivities of metallic strain gauges, CNT containing composites and other experiments conducted with SWCNT BPs (MWCNT weren't characterized electromechanically till now). [1, 2, 14, 15].
Each specimen that was characterized in the cyclic loading experiments was loaded till failure, as shown in Table 3.
The resistance change of SWCNT and MWCNT incorporated into polymer 1 are similar to the cyclic loading results (higher sensitivity of SWCNT sensor). Polymer 1 shows

very little inelastic change even at high strain, thus the behavior of the sensors didn't change for strains higher than 1%.
Results obtained for polymer 2, provides a remarkable insight into processes which govern the electromechanical properties of the BP strain sensors.
For MWCNT and SWCNT BP sensors the resistance changes with a relatively low sensitivity at lower strains (up to 7.5% and 5% respectively). At higher strains the sensors show a rise in sensitivity to strain. MWCNT sensors exhibit a relatively constant sensitivity to strain up to relatively high strains (more than 30%). This property allows using MWCNT BP as a sensitive strain sensor of relatively high strains.
On the other hand, SWCNT BP sensors show a different behavior at high strains, and could not practically function as strain sensors for strains beyond 15%.
This phenomenon is most probably caused by SWCNT BP failure and disruption of the conducting path, which cause an abrupt rise in the sensor's resistance.

Table 3 - Stress and Resistance change as a function of strain for different BP types and polymer matrices, loading till failure

	MWCNT BP sensor	**SWCNT BP sensor**
Polymer 1	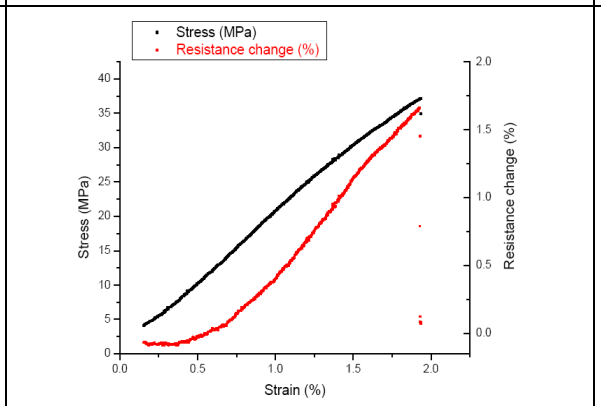	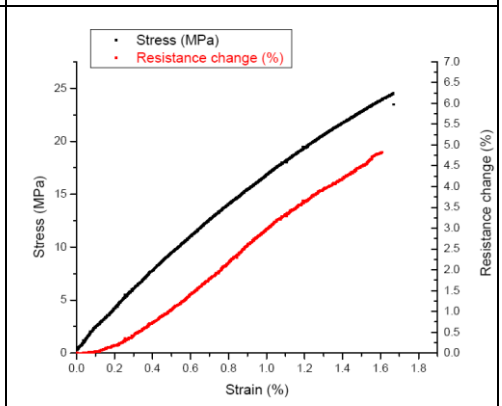
Polymer 2	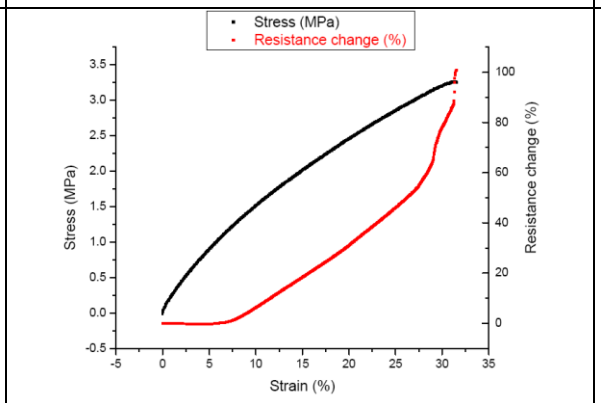	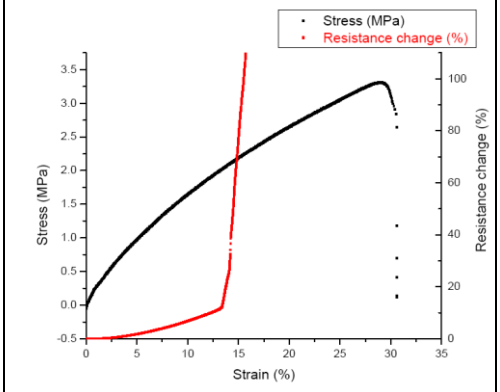

Since the volume fraction of the NT in the MWCNT BP sensor is lower than the volume fraction of SWCNT BP sensor, the mesh which is formed by the SWCNT is more rigid due to increased number of contacts, per unit volume.
The length that single-walled nanotubes are able to travel due to slippage is considerably less than multi walled nanotubes in the sensor, and this could explain the ability of MWCNT BP to sense very large strains.

Resistivity of MWCNT and SWCNT BP sensors

In order to understand the processes which govern the electromechanical properties the resistivity change as a function of strain should be calculated and referred to as the sensor physical property.

In order to calculate the resistivity from resistance data, we assume that the BP sensor is attached to the matrix, and do not disconnect from the polymer matrix.

The electrical resistivity ρ could be calculated from Ohm's law:

$$R = \rho \frac{L}{A} \quad (3)$$

where R is the electrical resistance of the sensor, ρ is the electrical resistivity, L is the length of the sample, and A is the cross-sectional area normal to the electron flow direction.

Upon extension, L increases, A decreases due to Poisson effect, and the sample resistance changes simply due to geometrical change. The resistivity is expected to remain constant, unless structural or morphological changes in the sensor occur. [16]

Since the specimens' length, L, is a function of the strain, we could find a simple relationship between the changes in resistance to the change in the resistivity as a function of strain:

$$\frac{\rho}{\rho_0} = \frac{R}{R_0} \cdot \frac{A_0(1-2\nu\varepsilon)}{L_0(1+\varepsilon)} \quad (4)$$

where ρ_0 is the initial resistivity of the sensor; R_0 is the initial resistance of the samples; ν – Poisson ratio, L_0 – the initial length of the sample, A_0 – the initial cross sectional area of the sample, ε – samples' strain.

Assuming that the contraction of the sensor was induced by the polymer matrix, the resistivity values of the BP sensors as a function of the strain was calculated using ν values obtained for the polymers (no gap between the sensor and the matrix was observed).

Table 4 – Resistivity change as a function of strain, for different BP sensors and polymer matrices

	MWCNT BP sensor	**SWCNT BP sensor**
Polymer 1	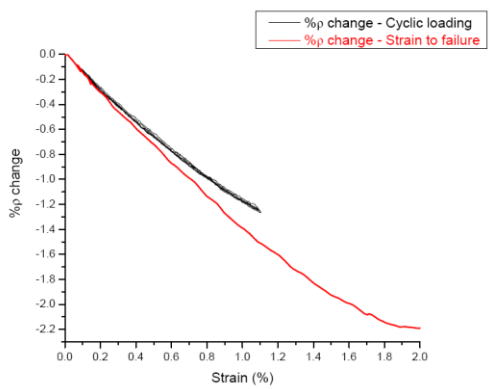	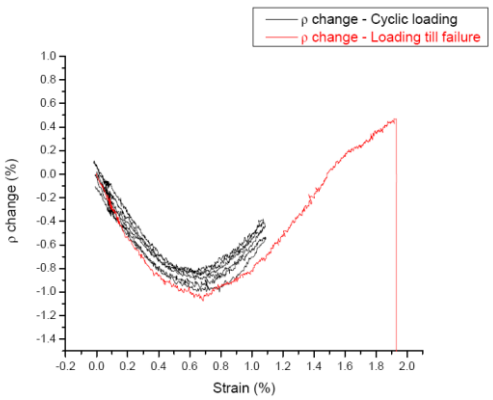

Polymer 2	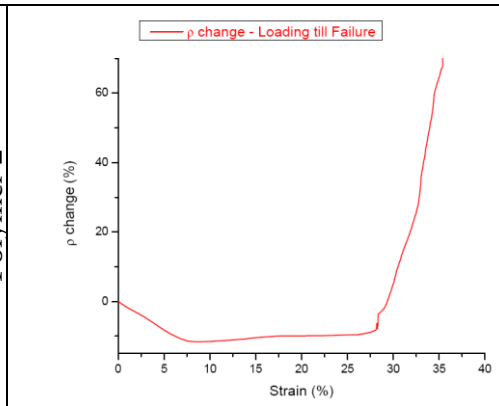	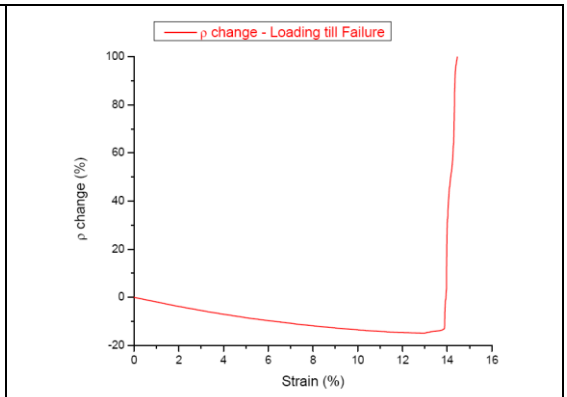

The resistivity change as a function of strain curves reveal that the change in the resistivity is a complex process, which is influenced by several mechanisms.

For low strains the resistivity decreases, where all polymer materials and both MWCNT and SWCNT exhibit this property.

We suggest that the resistivity decreases due to nanotube alignment in the BP sensor which causes an increase in contact area between current carrying nanotubes or nanotube bundles. It was previously shown by Wagner et. al. [17, 18] that mechanical strain can imply orientation of the tubes in the polymer. The orientation was readily obtained at relatively low strains, and upon each unloading the nanotubes seems to be reverted to their initial state, similar to the results obtained in this work, as shown in **Table** . Comparing the sensors incorporated into polymer 1, MWCNT BP sensor show a decrease in resistivity up to the failure of the specimen, which occurs at strain of ~2%. SWCNT BP sensor show decrease up to 0.6% of strain, and for higher strain, the electromechanical mechanisms changes, and the resistivity increases with strain.

The most probable cause to the resistivity increase is nanotubes slip and lose of overlapping contact with each other [14].

Polymer 2 shows the highest difference in properties between SWCNT and MWCNT BP sensors. As was previously seen, SWCNT sensor show extremely large change at strains considerably lower than for MWCNT sensor. This property is seen for resistivity values as well. Most probably, both sensors show an initial alignment of NT in the polymer causing resistivity decrease up to 6% of strain. The NTs in the SWCNT BP sensor continue to align up to strains of 14%, although the onset of contact release happens abruptly, and the resistivity increases very fast. NTs in the MWCNT start to slip one on another for strain higher than 7.5%, as could be explained by the relatively low change in resistivity up to 27% of strain. Consequently, lose of contacts happen for MWCNT sensor as well, for considerably higher strains.

CONCLUSIONS

The electromechanical properties of SWCNT and MWCNT were studied. The change of the resistance as a function of strain was assessed and the sensitivity of the sensors to strain was calculated. We had shown that both MWCNT and SWCNT BP sensors are sensitive to strain and possess sensing features. The BP sensors could measure strains of materials with different mechanical properties, and the sensitivity of SWCNT BP is higher relative to the sensitivity of MWCNT BPs. When comparing the results obtained for the different polymer matrices, the resistance change occurred in the same manner and degree for all polymer matrices, regardless to the stress applied on the material.

MWCNT BP showed remarkable sensing capabilities to strains up to 30% where as resistivity calculation revealed a complex deformation mechanism which suggests that carbon nanotubes are aligned in the polymer matrix at relatively low strains and then start to slip on each other.

REFERENCES

1. Dharap P., Li Z., Nagarajaiah S., and Barrera E.V. *Nanotechnology* **15** (2004), 379-382.
2. Kang I., Heung Y.Y., Kim J.H., Won Lee J., Gollapudi R., Subramaniam S., Narasimhadevara S., Hurd D., Kirikera G.R., Shanov V., Schultz M.J., Shi D., Boerio J., Mall S., and Ruggles-Wren M. *Composites: Part B* **37** (2006), 382-394.
3. Zhang W., Sakalkar V., and Koratkar N. *Applied Physics Letters* **91** (2007), 113102.
4. Kukovecz A., Smajda R., Oze M., Schaefer B., Haspel H., Konya Z., and Kiricsi I. *Physica Status Solidi (b)* **245** (2008), 2331-2334.
5. Maramatsu H., Hayashi T., Kim Y.A., Shimamoto D., Kim Y.J., Tantrakarn K., Endo M., Terrones M., and Dresselhaus M.S. *Chemical Physics Letters* **414** (2005), 444-448.
6. Xu G., Zhang Q., Zhou W., Huang J., and Wei F. *Applied Physics A: Materials Science and Processing*, **92** (2008), 531-539.
7. Ku C.L. MSc thesis, The Florida State University, 2007.
8. Lyons P.E., De S., Blighe F., Nicolosi V., Pereira L.F.C., Ferreira M.S., and Coleman J.N. *Journal of Applied Physics*, **104**, 044302-1 – 044302-8.
9. Bozhko A.D., Sklovsky D.E., Nalimova V.A., Rinzler A.G., Smalley R.E., and Fischer J.E. *Applied Physics A* **67** (1998), 75.
10. H., Wong W., and Lieber C.M. *Science* **272** (1996), 523.
11. Thess A., Lee R., Nikolaev P., Dai H., Petit P., Robert J., Xu C., Lee Y.H., Kim S.G., Rinzler A.G., Colbert D.T., Scuseria G., Tomanek D., Fischer J.E., and Smalley R.E. *Science* **273** (1996), 483.
12. Li H., Yin W.Y., Banerjee K., and Mao J.F. *IEEE Transactions on electron devices*, **55** (2008)
13. Hu N., Karube Y., Yan C., Masuda Z., and Fukunaga H. *Acta Materialia* **56** (2008), 2929-2936.
14. Park M., Kim H., and Youngblood J.P. *Nanotechnology* **19** (2008), 1-7.
15. Loh K.J., Kim J., Lynch J.P., Wong Shi Kam N., and Kotov N.A. *Smart Materials and Structures* **16** (2007), 429-438.
16. Pramanik P.K., Khastagir D., and Saha T.N. *Journal of Materials Science* **28** (1993), 3539-3546.
17. Zhao Q., and Wagner H.D. *Philosophy Transactions Royal Society London A* **362** (2004), 2407-2424.
18. Wood J.R., Zhao Q., and Wagner H.D. *Composites: Part A* **32** (2001), 391-399.